Scaled-energy spectra and closed classical orbits of the hydrogen atom in parallel electric and magnetic fields

Michael Courtney
Massachusetts Institute of Technology, 77 Massachusetts Avenue, Cambridge, Massachusetts 02139
(Received 31 January 1995)

Rydberg atoms in strong fields have scaling properties that allow detailed interpretation of photoabsorption spectra in terms of classical trajectories. The classical dynamics remains invariant if a spectrum is obtained at constant scaled energy. Since each orbit which is closed at the nucleus produces a sinusoidal modulation in the absorption spectrum, its signature is a peak in the Fourier transform of a scaled-energy spectrum. This paper identifies the effect of closed orbits in the computed spectrum of the hydrogen atom in parallel electric and magnetic fields in a region where chaos is just beginning to develop.

PACS number(s): 32.60.+i, 05.45.+b, 03.65.Sq

I. INTRODUCTION

Rydberg atoms in strong fields have attracted great interest as experimentally accessible quantum systems where the external perturbations can be comparable to the unperturbed energy [1]. The case of diamagnetism has been thoroughly explored both as a testing ground for quantum methods and as a laboratory for the study of quantum chaos [2]. The Stark effect is separable for hydrogen, but not for other atoms. Both quantum [3, 4] and semiclassical approaches [5] have been fruitful in describing phenomena in Stark systems. The problem of Rydberg atoms in parallel electric and magnetic fields adds a level of complexity because two external perturbations can be comparable to the unperturbed energy. Cacciani *et al.* [6] have fully explored the region where both fields are sufficiently small that levels from adjacent n manifolds do not overlap.

The spectra of Rydberg atoms under large perturbations can be complex and difficult to interpret. Scaled-energy spectroscopy [7, 8] has emerged as a valuable tool for interpreting these spectra in terms of classical trajectories which begin and end at the nucleus. According to closed-orbit theory [9], each closed orbit produces a sinusoidal modulation in the absorption spectrum. Early experiments observed the lowest period modulations by measuring photoabsorption spectra at fixed field [10]. Later experiments identified several of the lowest period orbits in the Fourier transform of a spectrum obtained at fixed field [11]. This approach is limited because the periods of closed orbits change over the energy range of the scan. However, classical scaling rules [12, 13] permit the energy and applied fields to be varied simultaneously to measure a spectrum in such a way that the classical dynamics of the system is invariant over the scan range. The Fourier transform of a scaled-energy spectrum is called a recurrence spectrum, because each peak corresponds to an orbit returning to the origin.

The effect of closed orbits has been identified in the continuum spectra of barium in parallel electric and magnetic fields [14], but the lack of scaled-energy spectroscopy limited the ability to resolve orbits, and the experimental resolution limited the study to short-period orbits. A separate study [15] has shown that qualitative spectral features in the continuum regime can be predicted from a purely classical analysis. Scaled-energy spectra of hydrogen in parallel fields have been computed previously in the quasidiscrete region [16], but the analysis identified recurrences associated with only a few short-period orbits. This paper presents a study of recurrence spectra in the discrete region where the fields are sufficiently strong that levels from many n's are mixed and where classical chaos is just beginning to develop. Computing scaled-energy spectra over a much larger field range than previous work gives highly resolved recurrence spectra. This permits identification of many recurrences and detailed interpretation of the spectra in terms of classical orbits.

II. SCALING RULES AND SYMMETRIES

According to closed-orbit theory [9], the photoabsorption cross section is given by a slowly varying background plus an oscillatory sum of the form

$$Df(E) = \sum_k \sum_{n=1}^{\infty} D_{nk} \sin(nS_k - \Phi_{nk}), \tag{1}$$

where k runs over all primitive closed orbits (orbits which are not repetitions), and n runs over repetitions of the primitive orbits. S_k is the action of the first repetition of a closed orbit. D_{nk} is the recurrence amplitude of each closed orbit. It contains information about the stability of the orbit, the initial and final angles of the orbit, and the matrix element of the dipole operator between the initial state and zero-energy Coulomb wave. Φ_{nk} is an additional phase which is computed from the Maslov index and related geometrical considerations. The square of the recurrence amplitude D_{nk} is the recurrence strength.

The Hamiltonians of Rydberg atoms in strong fields can be scaled so that the classical dynamics depends only on a scaled energy, not on the energy and field separately.

In the case of diamagnetism [12], the scaled energy is $\epsilon_B = EB^{-2/3}$, where E is the energy and B is the magnetic field. In the case of the Stark effect [13], the scaled energy is $\epsilon_F = EF^{-1/2}$, where F is the electric field. The classical actions scale as $S = 2\pi w\tilde{S}$, where w is the scaled field: $w_F = F^{-1/4}$ in the electric field case, and $w_B = B^{-1/3}$ for diamagnetism.

These scaling rules facilitate the study of recurrence spectra because the oscillatory component that each closed orbit contributes to the spectrum has a frequency $\tilde{S}$ if the photoabsorption spectrum is obtained as a function of w at constant scaled energy. The height of each peak in a recurrence spectrum is proportional to that orbit's recurrence strength. Consequently, in addition to providing a tool for computing spectra, closed-orbit theory is useful for interpreting spectra. In principle, one can identify the existence of classical orbits from the spectrum. From this point of view, closed-orbit theory constitutes a potentially powerful tool for predicting classical behavior from quantum structure.

Scaled-energy spectroscopy of the hydrogen atom in parallel electric and magnetic fields requires that two scaled energies be held constant. The Hamiltonian of hydrogen in parallel fields in the z direction is

$$H = \frac{p^2}{2} - \frac{1}{r} + Fz + \frac{1}{2}L_zB + \frac{1}{8}B^2\rho^2. \tag{2}$$

Applying the magnetic field scaling ($r = B^{-2/3}\tilde{r}$, $p = B^{1/3}\tilde{p}$) to the parallel field Hamiltonian gives

$$\tilde{H} = B^{-2/3}H = \frac{\tilde{p}^2}{2} - \frac{1}{\tilde{r}} + \frac{1}{2}\tilde{L_z} + \frac{1}{8}\tilde{\rho}^2 + FB^{-4/3}\tilde{z}. \tag{3}$$

The dynamics depends on $\epsilon_B = EB^{-2/3}$ and $FB^{-4/3}$. Notice that $FB^{-4/3} = (\epsilon_B/\epsilon_F)^2$, so using ϵ_B and ϵ_F is an equivalent way to parametrize the parallel field system.

This parametrization in terms of electric and magnetic scaled energies can be related to the parameter β used by Cacciani *et al.* to approach the parallel field system using tori quantization [6]. For small field values, hydrogen in parallel fields has an approximate symmetry which is a generalization of the Λ symmetry in diamagnetic hydrogen. The constant of motion can be written

$$\Lambda_\beta = 4A^2 - 5A_z^2 + 10\beta A_z, \tag{4}$$

where $\mathbf{A}$ is the Runge-Lenz vector and

$$\beta = \frac{12F}{5B^2n^2}. \tag{5}$$

β is related to the magnetic and electric field scaled energies as

$$\beta = \frac{24}{5}\frac{\epsilon_B^3}{\epsilon_F^2}, \tag{6}$$

where the substitution $E = -1/2n^2$ has been made.

In the low field region, spectra of hydrogen in parallel fields display very small anticrossings [16] as a consequence of the Λ_β symmetry. Furthermore, the symmetry allows the spectrum to be described in terms of three classes of eigenstates which correspond to the semiclassical quantization of three classes of trajectories. Classifying these eigenstates and the boundaries dividing the different classes allows for a complete description of the low field spectrum.

This paper considers spectra in regions where the fields are strong enough for there to be significant mixing among different n's. Computing scaled-energy spectra at $\epsilon_B = -0.6$ with $-\infty < \epsilon_F < -2$ (the classical ionization limit is $\epsilon_F = -2$) allows study of the spectral evolution in terms of classical orbits in the regime where classical chaos is just beginning to develop. (For pure diamagnetism, the system is near integrable for $\epsilon_B < -0.54$.) As ϵ_F is raised, the classical dynamics changes in a simple way which is easily seen in the recurrence spectra.

III. RECURRENCE SPECTRA

In the region of energies and fields considered here, it is sufficient to compute the spectrum by diagonalizing the Hamiltonian matrix in the spherical basis of hydrogenic eigenstates [18]. Eigenvalues and oscillator strengths are computed in a region around the desired scaled energy, and a spectrum at constant scaled energy is obtained by interpolation. In principle, the scaled-energy spectrum could be considered either a function of $w_F = F^{-1/4}$ or $w_B = B^{-1/3}$, the Fourier transform of which gives peaks at the scaled actions $\tilde{S}_F$ or $\tilde{S}_B$, respectively. The two possible recurrence spectra are equivalent and related by stretching the action axis. Here, the recurrence spectra are presented as a function of $\tilde{S}_B$ because of the close connections with diamagnetism. Before taking the Fourier transform of the oscillator strength spectrum to obtain a recurrence spectrum, the oscillator strength spectrum is multiplied by w_B^3 to remove the global variation of oscillator strength over the range of fields.

To interpret recurrence spectra, it is helpful to recall the basic structure of closed orbits in pure diamagnetic hydrogen. At large negative scaled energies, there are three primitive short-period closed orbits: one moves on the ρ axis, and two move on the $\pm z$ axis [12]. Most longer-period primitive closed orbits are created by bifurcations of these orbits and their repetitions as ϵ_B is increased. The orbits on the ρ axis and those which bifurcate from them are called *rotators*. Recurrences corresponding to these orbits will be labeled R_n^b, where n denotes the repetition of the orbit on the ρ axis from which the orbit bifurcated, and b distinguishes between different orbits which bifurcated from the same parent. The orbits on the z axis and those which bifurcated from them are called *vibrators*. Recurrences corresponding to these orbits are labeled V_n^b, where n and b have the same meaning as for the rotators.

Turning on a small electric field breaks the symmetry between the vibrators on each side of the z axis. The vibrators on the "uphill" side of the electric potential correspond to the class II motion described by Cacciani *et al.* [6]. The vibrators on the "downhill" side correspond to class I motion, and the rotators correspond to class III motion. All three classes of motion exist for sufficiently small electric fields. As the scaled electric field is raised, the region of phase space supporting the uphill vibrators

shrinks. At $\beta = 1/5$, class II motion ceases to exist, except for the orbit on the z axis in the uphill direction, which has become unstable. As ϵ_F is raised further, the region of phase space supporting class III motion shrinks. At $\beta = 1$, class III motion ceases to exist, and the uphill parallel orbit becomes stable again.

Recurrence spectra for $\epsilon_B = -0.6$ and $\epsilon_F = -3.0$ are shown in Fig. 1. (To enhance visibility of the smaller peaks, the square root of the power spectrum, or recurrence amplitude, is plotted.) Letters identify peaks as corresponding to the closed orbits listed in Table I and shown in Fig. 2. Repetitions have the number of repetitions as a prefix. The upper case letters U and D denote the uphill and downhill orbits on the z axis. In Fig. 2 orbits a–c are uphill vibrators (class II). Orbits d–n are rotators (class III), with l being a continuous deformation of the perpendicular orbit of pure diamagnetism. Orbits o–z and A–E are downhill vibrators (class I).

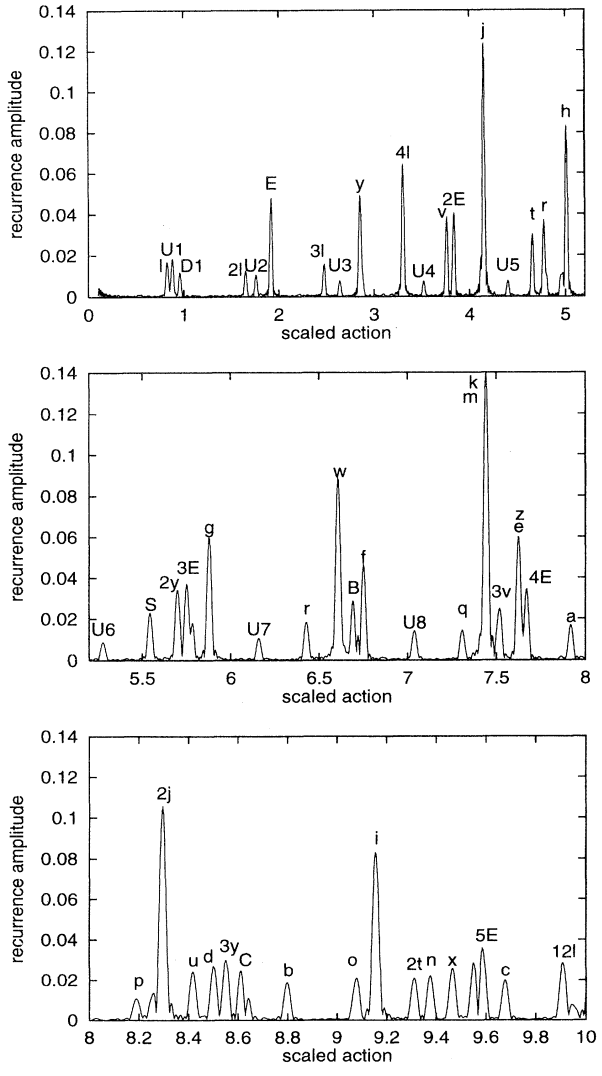

FIG. 1. Recurrence spectrum for $\epsilon_B = -0.6$, $\epsilon_F = -3.0$, $m = 0$, $3s$ initial state. Labeled peaks correspond to the closed orbits shown in Fig. 2 and Table I.

TABLE I. Closed orbits in parallel fields for $\epsilon_B = -0.6$ and $\epsilon_F = -3$. The labels are used in Figs. 1 and 2.

Orbit	θ_i (degrees)	$\tilde{S}_B$	Diamagnetic analog
U	0	0.880	V_1^+
a	6.99	7.921	V_9^1
b	9.15	8.803	V_{10}^1
c	10.27	9.678	V_{11}^1
d	14.58	8.501	R_{10}^1
e	15.88	7.627	R_9^1
f	17.84	6.754	R_8^1
g	20.91	5.880	R_7^1
h	25.99	5.013	R_6^1
i	29.93	9.160	R_{11}^2
j	35.74	4.151	R_5^1
k	45.67	7.446	R_9^2
l	80.87	0.831	R_1
m	111.88	7.445	R_9^2
n	128.92	9.381	R_{11}^1
o	130.03	9.063	V_{10}^1
p	130.45	8.198	V_9^1
q	131.07	7.311	V_8^1
r	132.07	6.430	V_7^1
s	133.69	5.549	V_6^1
t	136.31	4.656	V_5^1
u	138.19	8.419	V_9^2
v	140.63	3.764	V_4^1
w	143.82	6.618	V_7^2
x	145.05	9.465	V_9^3
y	148.16	2.855	V_3^1
z	152.12	7.633	V_8^3
A	154.46	4.778	V_5^2
B	157.37	6.696	V_7^3
C	158.89	8.631	V_9^5
E	165.62	1.921	V_2^1
D	180	0.959	V_1^-

The presence of the electric field causes the dynamics to differ dramatically from the case of pure diamagnetism. In pure diamagnetism at $\epsilon_B = -0.6$, the uphill and downhill vibrators are identical. Furthermore, the first three repetitions of the parallel orbit (V_1, V_2, and V_3) have not bifurcated. V_4 and higher have bifurcated at least once, but only V_8 and higher have bifurcated twice. If an electric field is applied so that $\epsilon_F = -3.0$, the bifurcations of the vibrators on the uphill side are greatly suppressed, and only V_9 and higher have bifurcated. In contrast, the applied electric field causes many more bifurcations to occur for the vibrators on the downhill side. V_2 and V_3 have both bifurcated giving V_2^1 and V_3^1 which correspond to the orbits E and y, respectively. These bifurcations do not occur in pure diamagnetism until the scaled energy is raised to approximately $\epsilon_B = -0.45$.

The rotators are also affected by the electric field. Many of them are skewed compared to their diamagnetic analogs, and orbits which were related to each other by reflection symmetry in pure diamagnetism are no longer symmetric (for example, k and m). In addition, for pure diamagnetism, R_4^1 had just been born by bifurcation at

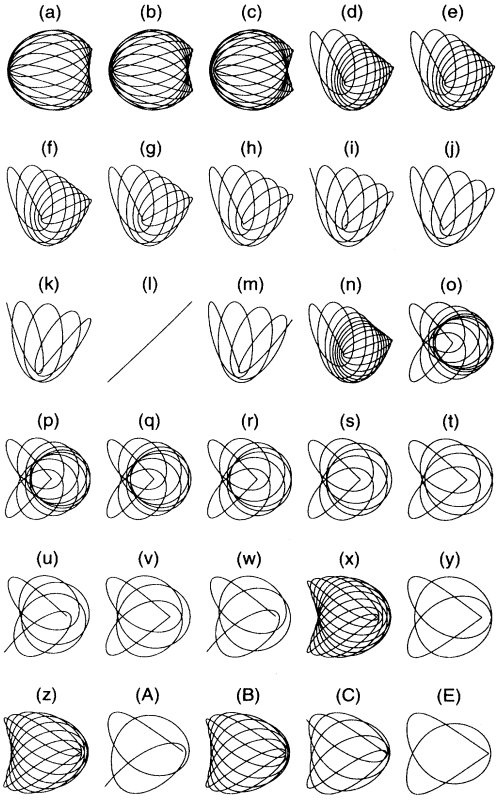

FIG. 2. Closed orbits for $\epsilon_B = -0.6$, $\epsilon_F = -3.0$, $L_z = 0$. Orbits are presented in order of increasing initial angle and are described in Table I.

$\epsilon_B = -0.6$. It does not exist for $\epsilon_F = -3.0$, but there is a strong focusing of the orbits close to $4l$ (whose diamagnetic analog is R_4) indicating that it is close to a bifurcation. The increase in recurrence strength which is typical near a bifurcation [12, 17] is present in $4l$, as shown in Fig. 1.

Figure 3 shows the evolution of recurrence spectra at $\epsilon_B = -0.6$ as ϵ_F is raised from $-\infty$ to -2. To compare recurrence amplitudes at different scaled energy ratios, the recurrence amplitude is plotted on the ϵ_B/ϵ_F axis. The general pattern is for more peaks to appear in the recurrence spectrum as ϵ_B/ϵ_F is raised. (Computational difficulties near the ionization limit produce a lot of "noise" in the recurrence spectrum for $\epsilon_B/\epsilon_F = -0.3$.)

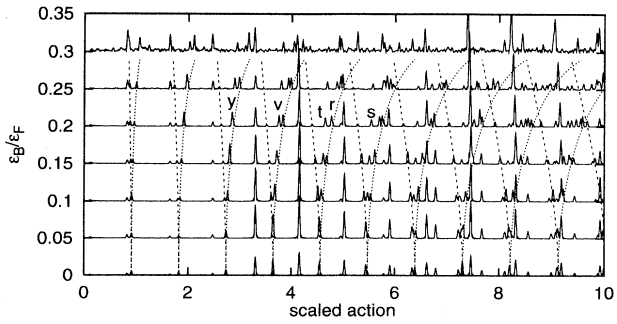

FIG. 3. Map of recurrence spectra for $\epsilon_B = -0.6$, $-\infty \leq \epsilon_F \leq -2$, $m = 0$, $3s$ initial state. The recurrence amplitude is plotted on the ϵ_B/ϵ_F axis. The long and short dashed lines are the actions of repetitions of the uphill and downhill orbits, respectively.

The reflection symmetry which exists for $F = 0$ is broken and the orbits on each side of the $z = 0$ plane differ in character, as discussed above. The splitting of the action of the parallel orbits is shown by the dashed lines in Fig. 3, and this splitting is also evident in the recurrence spectrum. New orbits are born by bifurcations of the downhill orbit. For example, the orbit labeled v in Figs. 1 and 2 is seen splitting off of the fourth repetition of the downhill parallel orbit as ϵ_F is increased. Recurrences labeled y, t, r, and S are also seen splitting off of repetitions of the downhill orbit as ϵ_F is raised.

IV. SUMMARY

In summary, analysis at constant scaled energy allows spectra of the hydrogen atom in parallel electric and magnetic fields to be interpreted in terms of classical orbits which are closed at the nucleus. The addition of an electric field to diamagnetic hydrogen tilts the potential surface so that orbits on the uphill side disappear and new orbits are created on the downhill side. These effects are clearly seen in the Fourier transform of spectra computed at constant scaled energy.

[1] T. F. Gallagher, *Rydberg Atoms* (Cambridge University Press, Cambridge, 1994); *Rydberg States of Atoms and Molecules*, edited by R. F. Stebbings and F. B. Dunning (Cambridge University Press, Cambridge, 1983), and references therein.

[2] H. Hasegawa, M. Robnik, and G. Wunner, Prog. Theor. Phys. **98**, 198 (1989); H. Friedrich and D. Wintgen, Phys. Rep. **183**, 38 (1989), and references therein; M. C. Gutzwiller, *Chaos in Classical and Quantum Mechanics* (Springer-Verlag, Berlin, 1990).

[3] E. Luc-Koenig and A. Bachelier, J. Phys. B **13**, 1769 (1980).

[4] D. Harmin, Phys. Rev. A **26** 2656 (1982).

[5] J. Gao and J. B. Delos, Phys. Rev. A **49**, 869 (1994); J. Gao, J. B. Delos, and M. Baruch, *ibid.* **46**, 1449 (1992); J. Gao and J. B. Delos, *ibid.* **46**, 1455 (1992).

[6] P. Cacciani, S. Liberman, E. Luc-Koenig, J. Pinard, and C. Thomas, J. Phys. B **21**, 3473 (1988); **21**, 3499 (1988); **21**, 3523 (1988); P. Cacciani and S. Liberman, Phys. Rev. A **40**, 3026 (1989).

[7] A. Holle, J. Main, G. Wiebusch, H. Rottke, and K. H. Welge, Phys. Rev. Lett. **61**, 161 (1988); T. van der Veldt, W. Vassen, and W. Hogervorst, Europhys. Lett. **21**, 9 (1993).
[8] U. Eichmann, K. Richter, D. Wintgen, and W. Sander, Phys. Rev. Lett. **61**, 2438 (1988).
[9] M. L. Du and J. B. Delos, Phys. Rev. Lett. **58**, 1731 (1987); Phys. Rev. A **38**, 1896 (1988); **38**, 1913 (1988).
[10] W. S. Garton and F. S. Tomkins, Astrophys. J. **158**, 839 (1969); A. Edmonds, J. Phys. (Paris) Colloq. **31**, C4-71 (1970).
[11] A. Holle, G. Wiebusch, J. Main, B. Hager, H. Rottke, and K. H. Welge, Phys. Rev. Lett. **56**, 2594 (1986).
[12] J. Main, G. Wiebusch, K. Welge, J. Shaw, and J. B. Delos, Phys. Rev. A **49**, 847 (1994).
[13] M. Courtney, H. Jiao, N. Spellmeyer, and D. Kleppner, Phys. Rev. Lett. **73**, 1340 (1994).
[14] J.-M. Mao, K. A. Rapelje, S. J. Blodgett-Ford, J. B. Delos, A. König, and H. Rinneberg, Phys. Rev. A **48**, 2117 (1993).
[15] M. A. Iken, F. Borondo, R. M. Benito, and T. Uzer, Phys. Rev. A **49**, 2734 (1994).
[16] K. Richter, D. Wintgen, and J. S. Briggs, J. Phys. B **20**, L627 (1987).
[17] M. Courtney, H. Jiao, N. Spellmeyer, D. Kleppner, J. Gao, and J. Delos, Phys. Rev. Lett. **74**, 1538 (1995).
[18] M. L. Zimmerman, M. G. Littman, M. M. Kash, and D. Kleppner, Phys. Rev. A **20**, 2251 (1979).